AIMS Materials Science

AIMS Materials Science, 11(1): 81–93.
DOI: 10.3934/matersci.2024004
Received: 26 October 2023
Revised: 30 November 2023
Accepted: 19 December 2023
Published: 02 January 2024

http://www.aimspress.com/journal/Materials

Research article

Results of experimental simulation of interaction between corium of a nuclear reactor and sacrificial material (Al_2O_3) with a lead layer

Mazhyn Skakov[1], Viktor Baklanov[2], Maxat Bekmuldin[2,3,*], Ivan Kukushkin[2], Assan Akaev[2], Alexander Gradoboev[4] and Olga Stepanova[3]

[1] National Nuclear Center of the Republic of Kazakhstan, Kurchatov 071100, Kazakhstan
[2] Institute of Atomic Energy NNC RK, Kurchatov 071100, Kazakhstan
[3] Shakarim University, Semey 071412, Kazakhstan
[4] National Research Tomsk Polytechnic University, Tomsk 634050, Russia

* **Correspondence:** Email: maks_alya@mail.ru; Tel: +7-771-547-5657.

Abstract: This paper presents the results of an experimental study of the interaction of a candidate sacrificial material (SM) for a light water reactor melt trap with corium at the Lava-B test-bench. The candidate sacrificial material is a combination of aluminum oxide and a lead layer. The idea of using such a combination of SM is based on the fact that when the lead layer interacts with corium, there will be an increase in the intensity of heat removal from the corium, as well as the chemical interaction between the corium and SM due to the high heat-conducting properties of lead. This approach will improve the efficiency of corium localization in the melt trap compared to the current set of sacrificial material. Experiments have shown active melting and boiling of lead during its interaction with corium. This is confirmed both by the readings of thermocouples and by the X-ray diffraction phase analysis of the deposit material formed on the walls of the melt receiver (MR) of the Lava-B bench, sampled after the experiment. The experiment results show that the lead layer reduces the rate of increase in the temperature of the corium and increases the rate of erosion of the ceramic part of the SM. With these circumstances, it is possible to conclude that the use of aluminum oxide with a lead layer is promising in practice.

Keywords: corium; severe accident; sacrificial material; core; induction heating; Lava-B bench

1. Introduction

Severe accidents of pressurized water reactors of nuclear power plants (NPPs) are accompanied by melting of the core and the formation of corium-a melt of a radioactive mixture of uranium oxide, zirconium, steel, products of the interaction of metals with an oxidizing environment, and other structural elements. The release of corium, under certain conditions, outside the reactor facility is considered as a possible scenario due to the large amount of stored energy and the presence of decay heat [1].

Currently, there are two options for localizing the core melt inside the containment during a severe accident at a NPP with light water reactors under pressure: in-vessel and out-of-vessel containment of the melt [2]. At the same time, the most acceptable method at the moment for managing the final stage of a severe accident with a core meltdown at NPPs with high-power reactors (over 1000 MW) is the concept of containing and cooling the corium outside the reactor vessel. This concept consists of installing a melt localization device (melt trap) in the sub-reactor space [3].

During its development, the concept of melt traps had moved from a simple pool filled with water to complex structures that combine many unique engineering solutions [4–8]. Currently, melt traps are known for light water reactors: evolutionary power reactor (EPR) [9], European Union advanced boiling water reactor (EU-ABWR) [10], economic simplified boiling water reactor (ESBWR) [11], European Union advanced power reactor (EU-APR) [12], water–water energetic reactor (WWER) [13], etc. One of the most technically feasible and often used melt traps is the crucible-type melt trap of the WWER reactor.

A crucible-type melt trap is a steel housing that forms a vessel in which a bath of corium melt coming from the core is formed. Cooling of the melt pool formed in the trap occurs by heat removal to the cooling water through the shell of the steel housing, as well as by water supplied directly to the surface of the melt after completion of gravitational inversion of the corium layers.

The main element of the gravitational inversion concept is sacrificial materials. The role of sacrificial materials is to dilute the heat-generating oxide part of the corium in order to create thermodynamic conditions for gravitational inversion of parts of the corium and reduce the high temperature [14].

Based on a set of experiments to justify the use of the first such trap at the Tianwan NPP, the use of ceramic materials as sacrificial materials was recommended. Experiments confirmed the eutectic nature of the phase diagrams formed by a multicomponent core melt with Al_2O_3 and Fe_2O_3. It was shown that the mutual dissolution of the sacrificial material and the melt occurs at a rate sufficient to implement the inversion of the oxide and metal layers in less than 1 hour. As a result, an oxide ceramic sacrificial material was synthesized, consisting of 67 wt.% Fe_2O_3 and 30 wt.% Al_2O_3 [15].

However, in the process of further research it was found that the selected materials have disadvantages, among which the following can be identified [16,17]:

- Heat removal from the corium by the bulk of sacrificial materials is not fully justified due to the low thermal conductivity of sacrificial materials ($\lambda = 0.5$ W/m·K);

- Release of oxygen during the decomposition of Fe_2O_3 will create a barrier gas-liquid layer that prevents heat and mass transfer.

Thus, the search for new sacrificial materials for melt traps is an urgent task. As an example, it is possible to note the latest experiments on the study of candidate oxide and concrete sacrificial materials [18,19].

To improve the efficiency of using sacrificial materials and eliminate the above-described disadvantages, it was decided to apply the previously conducted studies on the selection of material for a core catcher similar to the Tianwan NPP. Thus, in the original version, steel was considered as a sacrificial material, but the calculations and experimental studies performed showed that if only metal is used as a sacrificial material, then the thermal loads to the side cooling surfaces in the area where the oxide melt bath is located may exceed permissible values due to the limited depth and high-volume energy release densities [20]. Ultimately, experts concluded that the use of metal as SM is promising only in combination with an oxide sacrificial material.

Previously, in [21], to eliminate the above disadvantages, the authors proposed to consider a ceramic material made of aluminum oxide (Al_2O_3) with a lead layer (fluidized bed) as a sacrificial material. Computer simulation in the Ansys program showed that, due to the heat transfer from the corium to lead phase transitions, the growth rate of the average temperature of the corium decreases due to decay heat. At the same time, the interaction between lead and the sacrificial material leads to an increase in the intensity of heat exchange processes compared to the interaction between corium and the sacrificial material. This fact can lead to accelerated destruction of the sacrificial material and its further dissolution in the corium for the successful completion of gravitational inversion.

However, the disadvantage of the computer simulation is that it only takes into account the thermophysical interaction between the elements of the trap. Thus, the purpose of this study, in order to understand all aspects of such interaction, is to conduct physical simulation of the interaction between corium and ceramic material made of aluminum oxide and a lead layer under conditions of simulating decay heat in corium.

2. Materials and methods

Experiments on the interaction between corium and sacrificial material were conducted in the Lava-B test-bench [22–25]. Figure 1 shows the physical form and layout of the Lava-B facility. The experimental facility includes two main functional blocks: an electric melting furnace (EMF) for preparing the corium and a melt receiver (MR), which houses an experimental section for modeling the studied processes.

Before the start of the experiment to obtain corium, an electric melting furnace (EMF) crucible with a total mass of 25.5 kg was loaded with the following composition: UO_2: 16.5 kg; Zr: 7.5 kg; ZrO_2: 1.5 kg [26]. To add a steel component to the corium and eliminate the negative effect of carbon on its composition, a steel element (brand 12X18H10T: X—chromium, H—niccolum, T—titanium) with a developed interaction surface weighing 4.5 kg was installed in the concrete trap. Disks and cylinders made of aluminum oxide ($A1_2O_3$, purity 99 %) were installed in the internal cavity of the concrete trap. A general view of the core catcher with the studied samples is shown in Figure 2.

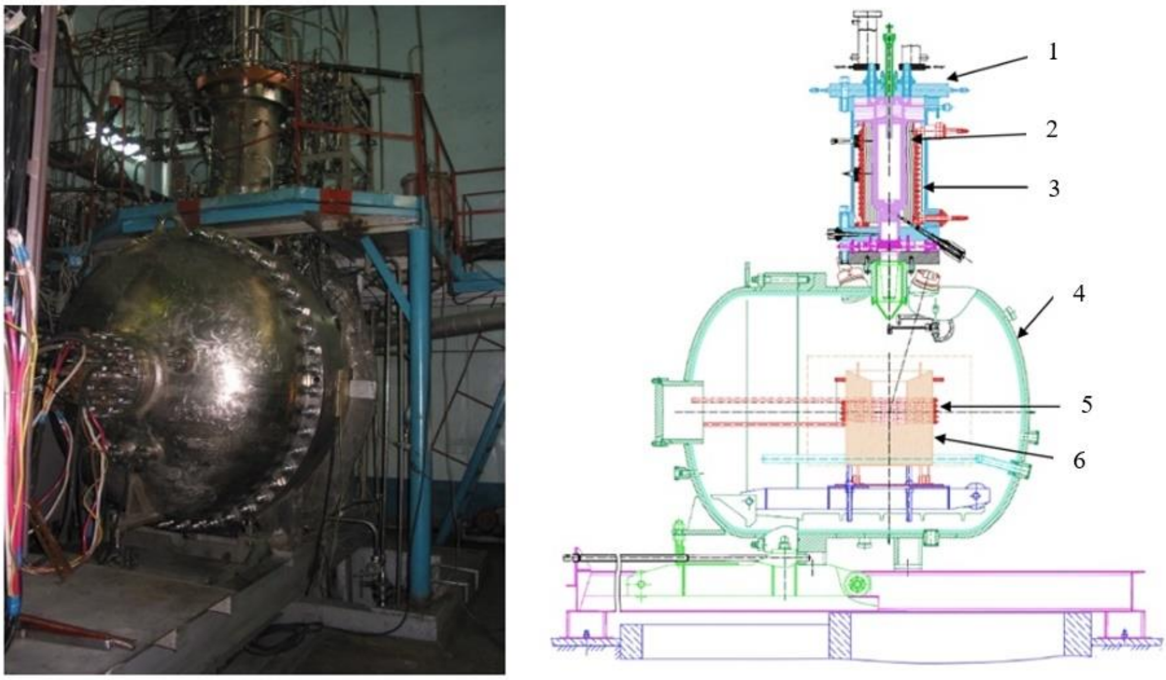

1—electric melting furnace (EMF); 2—crucible; 3—EMF inductor; 4—melt receiver (MR); 5—MR inductor; 6—concrete trap

Figure 1. Physical form and layout of the Lava-B facility.

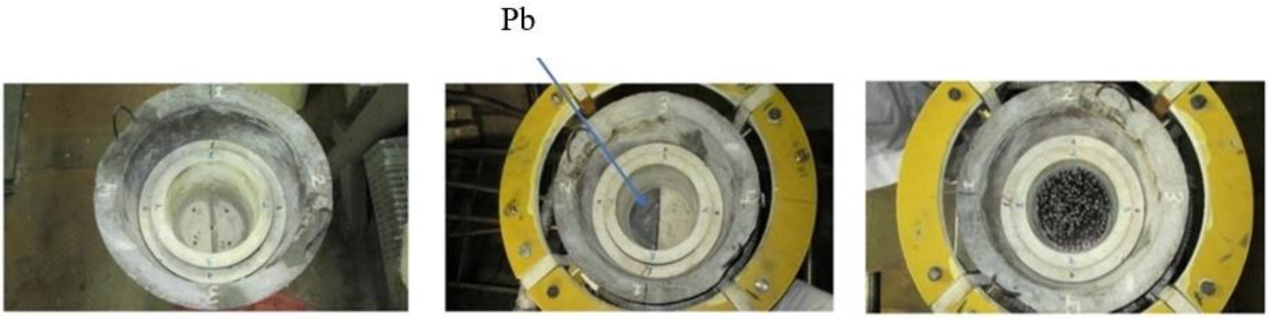

(a) (b) (c)

Figure 2. Installation of trap elements: (a) blocks and cylinders from $A1_2O_3$; (b) lead liner; (c) steel liner.

Figure 3 shows a diagram of the arrangement of thermocouples (tungsten–rhenium type with measurement error of 0–7%) in the core catcher with the dimensions of the concrete trap, blocks and cylinders made of $A1_2O_3$, and a lead liner (dimensions in the figure are in mm.). The routing of the compensation wires of the thermocouples of the concrete trap from the platform to the MR cover is made inside pipes made of corrosion-resistant steel.

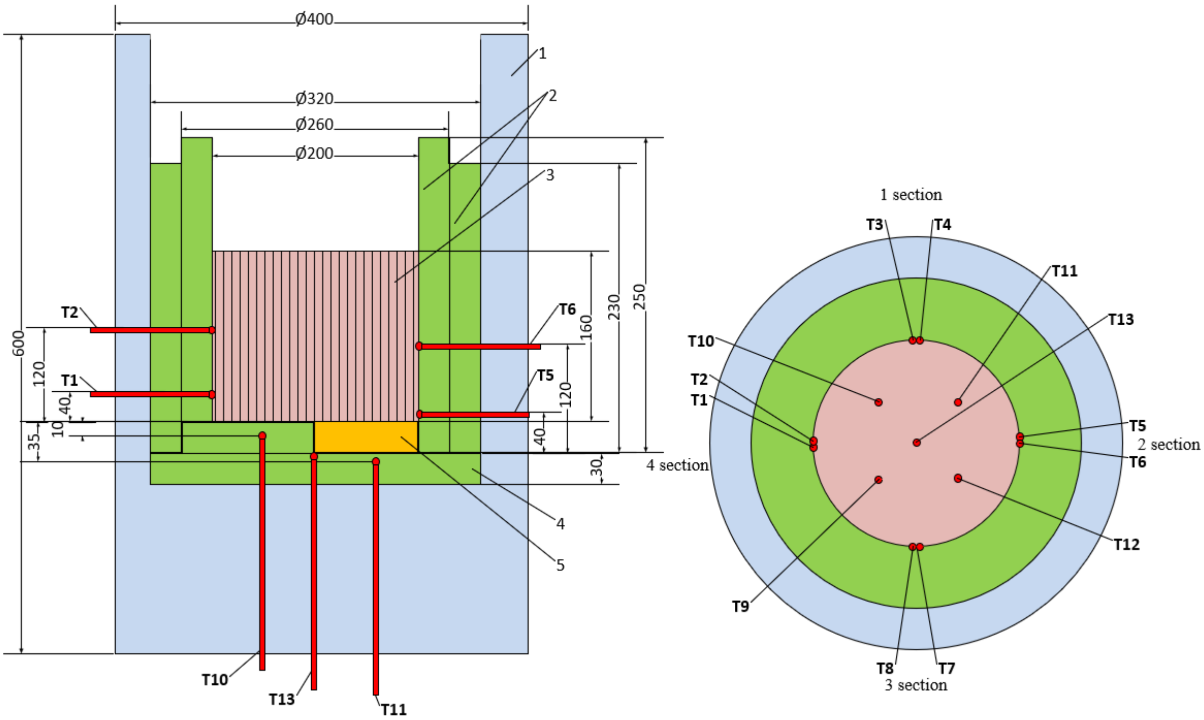

Figure 3. Diagram of the arrangement of thermocouples in a concrete trap: 1: concrete trap; 2: aluminum oxide cylinders; 3: steel liner; 4: aluminum oxide disc; 5: lead liner.

Next, the corium components were heated in an EMF crucible until a liquid state. The amount of integrated energy supplied to the EMF crucible was 367.4 MJ after 6960 s while the melt temperature, according to the infrared pyrometer readings, was about 2514 °C. Then, the voltage on the EMF inductor was reduced to 0 V and the crucible plug was chipped in order to move the corium into the core catcher.

After the melt was drained into the trap, voltage was applied to the MR inductor to simulate the decay heat in the corium. The method for selecting the parameters of the induction system in the MR and the results of previously conducted calibration experiments are described in detail in [27].

The interaction between corium and studied materials with the simultaneous input of extra energy into the melt lasted for 2700 s. The experiment was stopped when most of the controlling thermocouples failed. After turning off the power, the experimental device was cooled due to heat leakage into the MR elements of the Lava-B bench.

3. Results and discussion

The temperature of the experimental device (ED) during the experiment is shown in Figures 4 and 5. Figure 4 evidences that after the corium is moved into the trap, its active interaction with the sacrificial material begins, which is expressed by an increase in the temperature of the aluminum oxide blocks. At the same time, taking into account the reading of thermocouple T4, which is commensurate with the value of the melting point of aluminum oxide, it can be assumed that in the area where this thermocouple is located, melting of aluminum oxide occurred in the process of interaction with corium. Thermocouple T4 is located at the junction of areas with and without a lead layer. In the course of further research, the maximum erosion of aluminum oxide ceramics will occur and a sample for materials science research will be selected from this area.

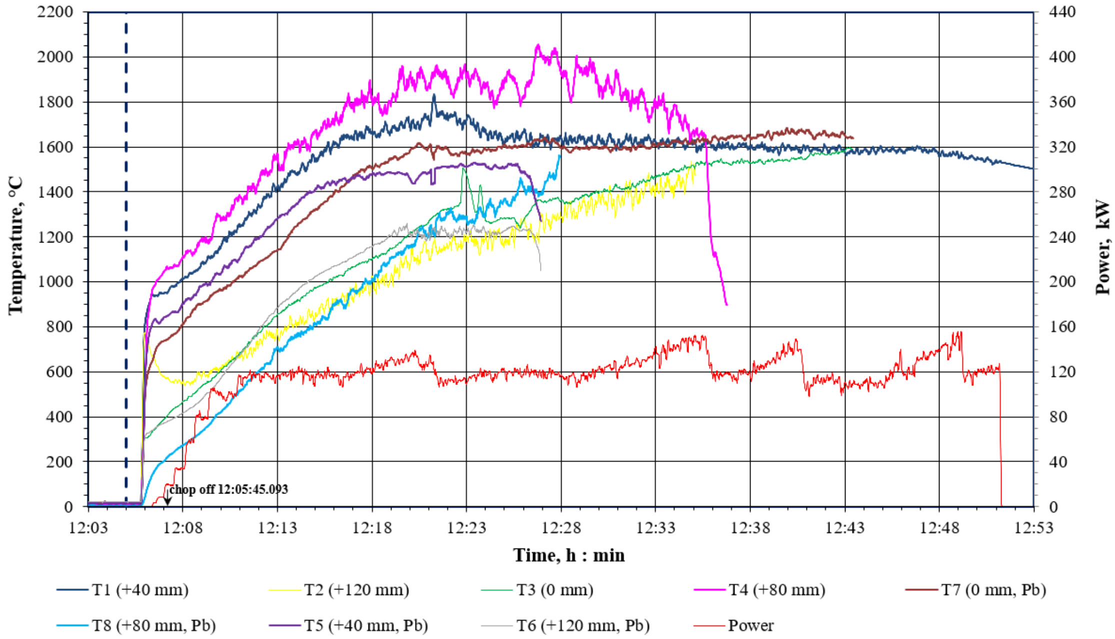

Figure 4. Diagrams of changes in temperature values during the interaction of the melt with Al_2O_3 (thermocouples in the side wall T1–T8).

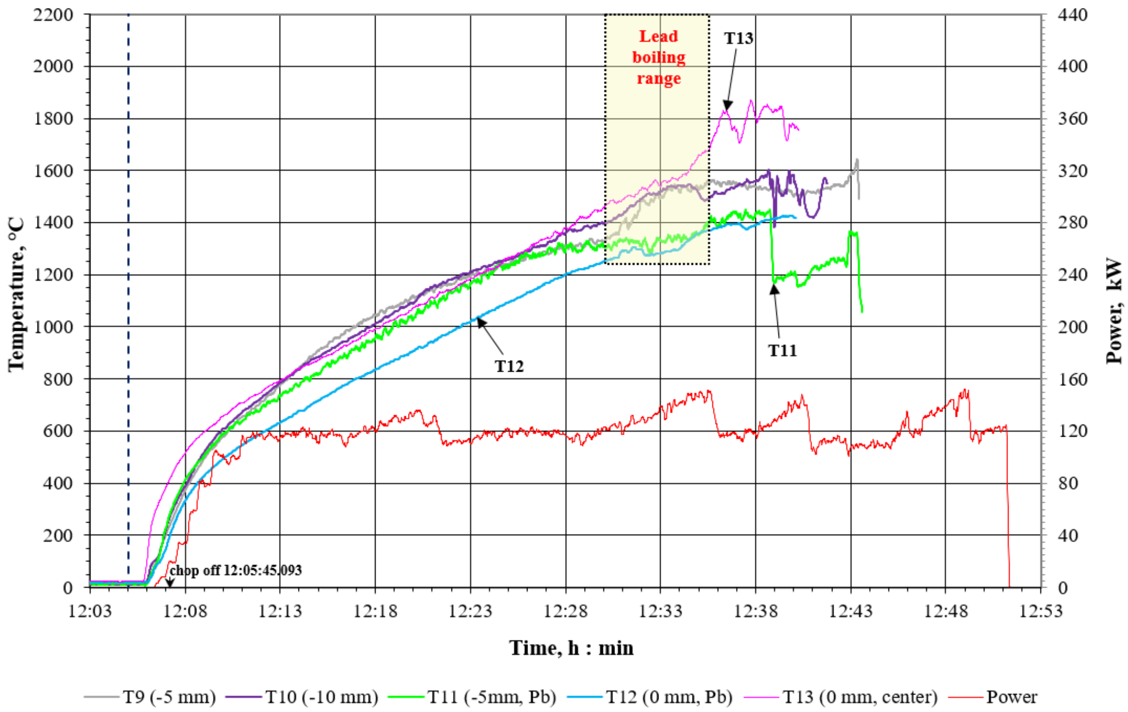

Figure 5. Diagrams of changes in the temperature values of the disks during the interaction of the melt with Al_2O_3 and the lead layer (thermocouples T9–T13).

At the same time, according to the results of the experiment, the readings of thermocouples installed in ceramic disks, not closed (thermocouple T13, Figure 5) and closed with the lead layer (thermocouple T11, Figure 5), differ significantly after the start of boiling and evaporation of lead. The rate of increase in temperature of the ceramic disk under the lead layer is lower. The boiling of the lead layer is also confirmed, as a later analysis showed, by the presence in the MR chamber and on the surface of the core catcher of particles of material with a diameter of 1–10 mm (Figure 6) after the experiment, visually identified as lead, presumably deposited during the condensation of metal vapors.

Figure 6. Fragments of detected material in the MR chamber and on the surface of the trap.

X-ray diffraction phase analysis was implemented to more accurately determine the composition of the material. Analysis of the diffraction pattern showed (Figure 7) that the main component of the phase composition is metallic lead. All the main intense peaks of the diffraction pattern correspond to this phase.

To obtain data on the interaction between corium and ceramic material (aluminum oxide), a diametrical section of the core catcher was made, which showed the presence of corium penetration beyond the original boundary of the side walls of the ceramic material to various depths (penetrating erosion). It was revealed that in the cross section of the trap, the depth of erosion of the side wall was maximum on the side containing lead, minimal on the side without a lead layer, and there was through erosion on the bottom disks and part of the concrete trap material in the entire section. For subsequent microstructural studies, it was necessary to obtain templates containing the pattern observed in the cross section. In this regard, it is supposed to make an additional diametrical cut in half of the trap and subsequent cutting of the plates.

From the quarters of the trap obtained after the additional cut, templates in the form of plane-parallel plates were cut along the entire height of the trap. Cutting a plate about 30 mm thick from a quarter of a trap containing lead was not successful, since during the cutting process the plate broke up into many fragments. From the part of the trap that did not contain lead, a more massive sample with a thickness of about 50 mm was cut out, located at the junction of both zones (without a layer of lead and with lead). By increasing the thickness of the template, it was possible to maintain its overall integrity. The cut plate contains a representative cross-sectional area of the trap with maximum sidewall erosion and metal accumulation detected (Figure 8).

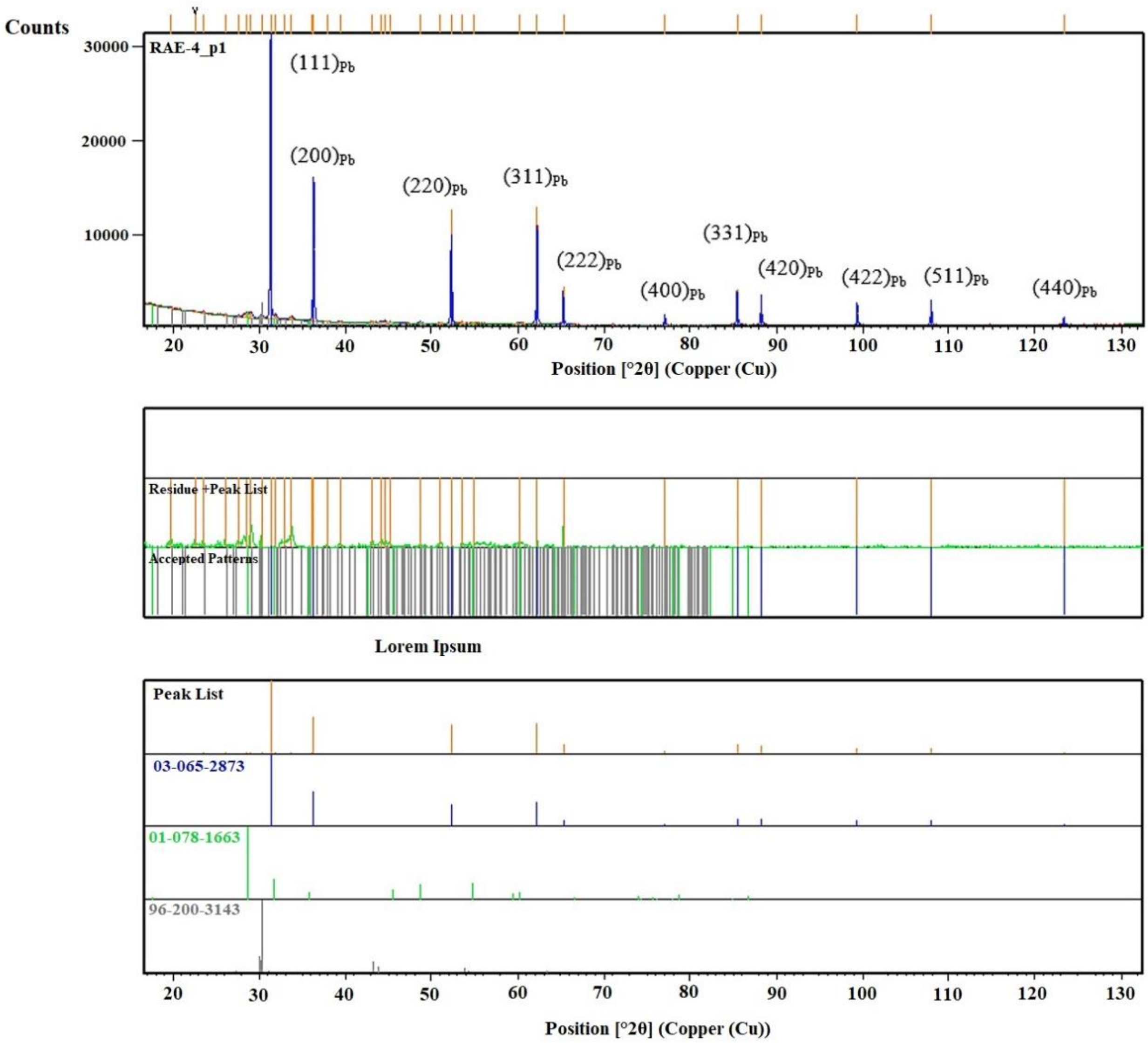

Figure 7. The result of X-ray diffraction phase analysis of detected material in the MR chamber and on the surface of the trap.

As can be seen, on the cut-out plate there are areas of through erosion of the internal insert, local penetration of the melt into the gap between the internal and external liners, and partial local erosion of the material of the external ceramic liner.

The choice of area for studying changes in structure was determined by searching for a fragment containing all the characteristic signs of erosion of ceramic material, i.e., the presence of an area of erosion, the presence of changes in structure, and cracks in ceramic liners. For further materials science research, the workpiece was cut into three plates about 15 mm thick. The plate cutting diagram and sample markings are shown in Figure 9.

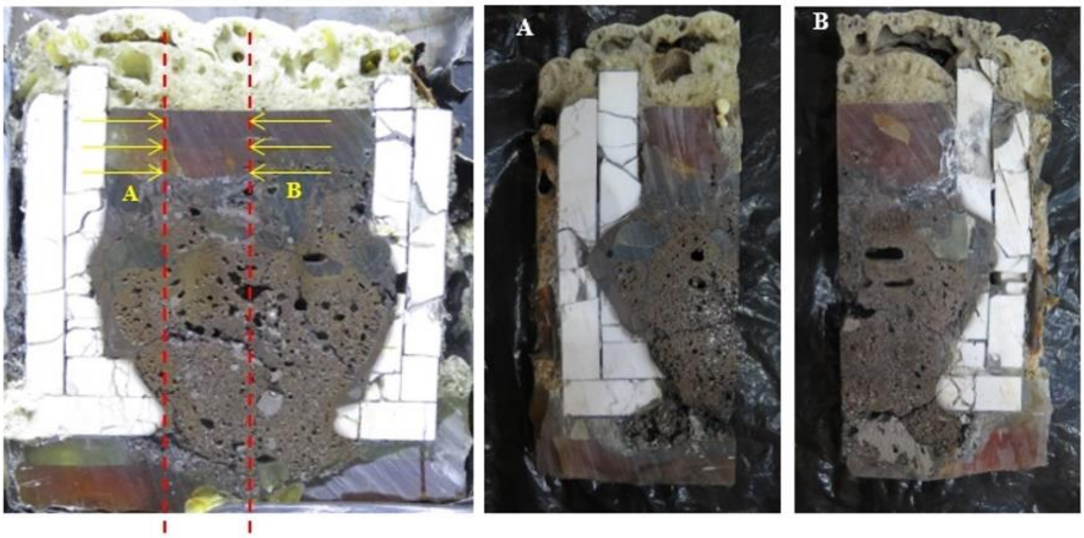

(a) (b)

Figure 8. Location (a) and appearance (b) of the surfaces of the sample cut from the trap.

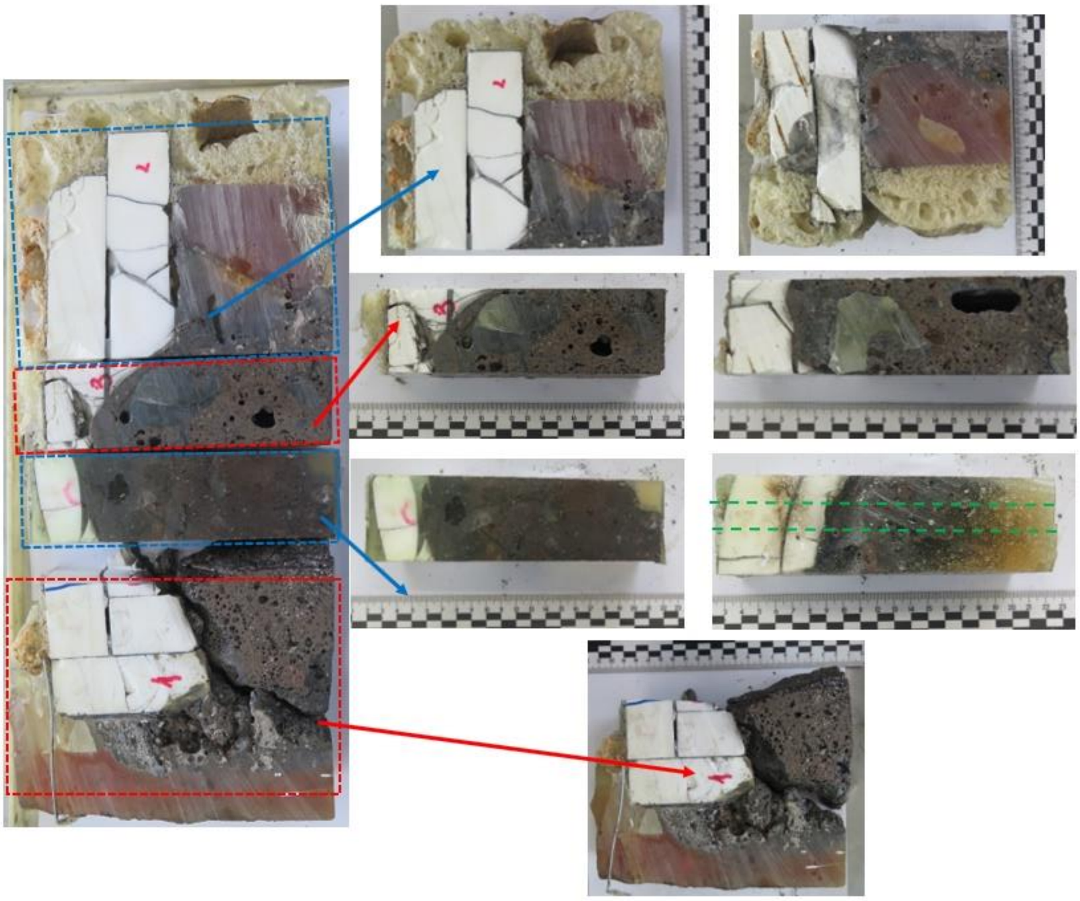

Figure 9. Scheme of cutting a plate for materials science research.

For materials science research, a thin section was made, including the area of maximum erosion of the ceramic material (Figure 10). The prepared section contains a close-to-diametrical cut of materials in the area of contact between the corium and the ceramic material.

Along with the obvious erosion boundary characterized by a sharp transition from the structure of the corium melt to the structure of the ceramic material, the area of influence of the melt on the ceramic material is also the area of visible preserved structure of the aluminum oxide material at different distances from the boundary with the melt. Indicators property degradation (mediated, secondary and indirect erosion) are signs of changes in the structure of a ceramic material, determined by optical macroanalysis, microstructural studies, and studies of strength properties.

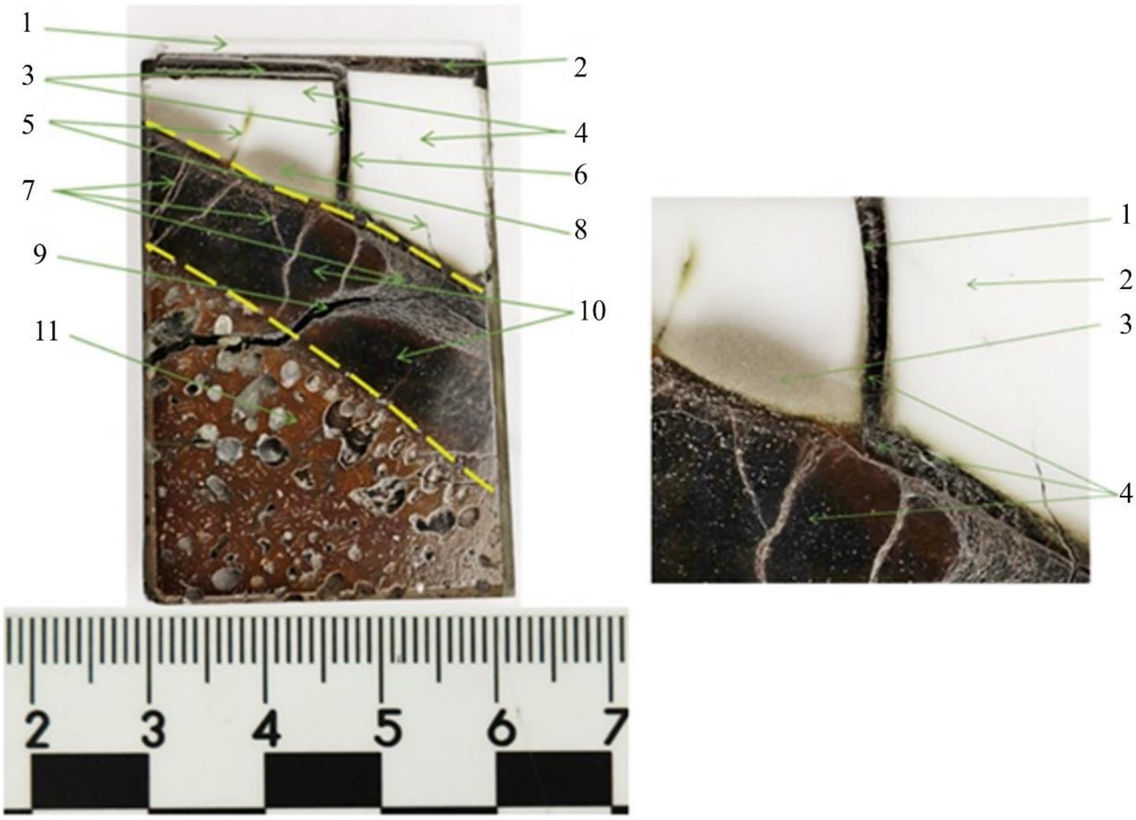

(a) (b)

Figure 10. Appearance of a sample for materials science research. a: 1—external liner of ceramic material; 2—epoxy; 3—corium with dark structure; 4—inner liner of ceramic material; 5—microcracks in the structure of ceramic material; 6—macrocrack in the structure of ceramic material; 7—microcracks in the structure of corium; 8—the area of darkening of the structure of the ceramic material; 9—microcrack in the structure of corium; 10—corium with dense dark structure; 11—corium with porous colored structure; b: 1—macrocrack in the structure of ceramic material; 2—inner liner of ceramic material; 3—the area of darkening of the structure of the ceramic material; 4—corium with dark structure.

The prepared section (see Figure 10a) contains an area of erosion of the ceramic material, areas of darkening of the structure (8), microcracks (5), macrocracks (6), and areas of corium penetration into the gap between the liners and into the macrocrack (3) in the ceramic material formed during the experiment. The structure of the corium and ceramic material also contains macrocracks (9), which were formed either during the processes of dismantling the trap and cutting out the workpieces or during the cooling of the assembly in the post-experimental period, at least after the melt solidified. A layer of solidified corium melt with a thickness of about 1 cm near the contact boundary with the ceramic material has a dense homogeneous structure (10), different from the structure of corium in the rest of the section (11), which is characterized by porosity and the presence of round metal inclusions.

4. Conclusions

In this study, we conducted an experiment to study the interaction of a candidate SM with corium under conditions as close as possible to the real processes of a severe light water reactor accident, i.e., using an aluminum oxide SM with a lead layer in the melt trap.

The experiment showed that during the interaction between corium with SM, melting and subsequent boiling of the lead component took place. These processes are confirmed by thermocouple readings and the presence of lead in the MR chamber and on the surface of the trap. In this case, when the boiling point of lead is reached, the rate of increase in the temperature of the ceramic material slows down over a certain time interval. This is most likely caused by phase transitions in the lead layer.

It was also found that the presence of lead increases the intensity of erosion of the oxide component of SM. Thus, the depth of side wall erosion turned out to be maximum on the side containing lead and minimal on the side without lead.

As a result of the destruction of the oxide part structure of the SM, its active introduction into the composition of the corium occurred. It was noticed that the layer of solidified corium melt near the contact boundary with the ceramic material had a dense homogeneous structure, different from the structure of the corium in the rest of the section, which was characterized by porosity and presence of round metal inclusions.

Thus, the experiment showed the perspective of the proposed combination of sacrificial materials for the melt trap. During future materials research, the processes of interaction between corium and the proposed SM will be studied in detail and conclusions will be drawn about the possibility of its use in melt traps of a light water reactor.

Use of AI tools declaration

The authors declare they have not used Artificial Intelligence (AI) tools in the creation of this article.

Acknowledgments

This research was funded by the Ministry of Energy of the Republic of Kazakhstan (BR09158470).

Conflict of interest

The authors declare no conflict of interest.

References

1. Harutyunyan R (1990) Chinese syndrome. *Nature* 11: 35–41.
2. Fischer M, Bechta S, Bezlepkin V, et al. (2017) Core melt stabilization concepts for existing and future LWRs and associated research and development needs. *Nucl Technol* 196: 524–537. https://doi.org/10.13182/NT16-19
3. Khabensky V, Granovskii V, Bechta S (2009) Severe accident management concept of the VVER-1000 and the justification of corium retention in a crucible-type core catcher. *Nucl Eng Technol* 41: 561–574. https://doi.org/10.5516/NET.2009.41.5.561
4. Song J, Suh N (2009) An evolution of molten core cooling strategies. *Nucl Eng Des* 239: 1338–1344. https://doi.org/10.1016/j.nucengdes.2009.02.010
5. Fish J, Piltch M, Arellano F (1982) Demonstration of passively-cooled particle-bed core retention. Proceedings of the LMFBR Safety Topical Meeting, Lyon, France, 327–336.
6. Turrichia A (1992) How to avoid molten core/concrete interaction (and steam explosions). Proceedings of 2nd OECD(NEA)CSNI Specialists Meeting of Molten Debris-Concrete Interaction, Karlsruhe, 503.
7. Fieg G, Möschke M, Werle H (1995) Studies for staggered pans core catcher. *Nucl Technol* 111: 331–340. https://doi.org/10.13182/NT95-A15863
8. Tromm W, Alsmeyer H (1995) Experiments for a core catcher concept based on water addition from below. *Nucl Eng Des* 157: 437–445. https://doi.org/10.1016/0029-5493(95)01000-8
9. Fischer M (2004) The severe accident mitigation concept and the design measures for core melt retention of the European pressurized reactor (EPR). *Nucl Eng Des* 230: 169–180. https://doi.org/10.1016/j.nucengdes.2003.11.034
10. Hamazaki R, Nakagawa T, Katagiri N, et al. (2011) Evaluation on core melt retention in core catcher of Toshiba's EU-ABWR. Proceedings of the International Congress on Advances in Nuclear Power Plants (ICAPP), Nice, France, 11414.
11. Lee J, Kim J, Kim T, et al. (2017) Overview of ex-vessel cooling strategies and perspectives. Proceedings of Transactions of the Korean Nuclear Society Spring Meeting Jeju, Korea, 1–5.
12. Song K, Nguyen T, Ha K, et al. (2017) Experimental study on two-phase flow natural circulation in a core catcher cooling channel for EU-APR1400 using air-water system. *Nucl Eng Des* 316: 75–88. https://doi.org/10.1016/j.nucengdes.2017.03.009
13. Kukhtevich I, Bezlepkin V, Granovskii V, et al. (2001) The concept of localization of the corium melt in the ex-vessel stage of a severe accident at a nuclear power station with a VVER-1000 reactor. *Therm Eng* 48: 699–706.
14. Gusarov V, Almyashev V, Beshta S, et al. (2001) Sacrificial materials for safety systems of nuclear power stations: A new class of functional materials. *Therm Eng* 48: 721–724.
15. Stolyarevsky A (2014) The problem of retaining molten fuel in the containment NPPs with WWER. *ISJAEE* 6: 25–35. Available from: https://www.isjaee.com/jour/article/view/437?locale=en_US.

16. Asmolov V, Bechta S, Berkovich V, et al. (2005) Crucible-type core catcher for VVER-1000 reactor. Proceedings of the American Nuclear Society-International Congress on Advances in Nuclear Power Plants, 1221–1227.
17. Asmolov V, Zagryazkin V, Isaev I, et al. (2002) Choice of buffer material for the containment trap for VVÉR-1000 core melt. *At Energy* 92: 5–14. https://doi.org/10.1023/A:1015094327731
18. Song J, Kim H, Hong S, et al. (2016) A use of prototypic material for the investigation of severe accident progression. *Prog Nucl Energ* 93: 297–305. https://doi.org/10.1016/j.pnucene.2016.09.003
19. Komlev A, Almjashev V, Bechta S, et al. (2015) New sacrificial material for ex-vessel core catcher. *J Nucl Mater* 467: 778–784. https://doi.org/10.1016/j.jnucmat.2015.10.035
20. Morozov A, Remizov O (2012) *Severe Accidents at NPPs with WWER: Scenarios, Core Degradation Processes, Control Methods: Textbook*, Obninsk: National Research Nuclear University MEPHI, 90–93. Available from: https://elib.biblioatom.ru/text/morozov_tyazhelye-avarii-na-aes_2012/p0/.
21. Bekmuldin M, Skakov M, Baklanov V, et al. (2021) Heat-resistant composite coating with a fluidized bed of the under-reactor core catcher of a light-water nuclear reactor. *Eurasian Phys Tech J 18*: 65–70. https://doi.org/10.31489/2021No3/65-70
22. Nazarbayev N, Shkolnik V, Batyrbekov E, et al. (2017) *Scientific, Technical and Engineering Work to Ensure the Safety of the Former Semipalatinsk Test Site*, London: Worldwide Promedia, 3: 296–298.
23. Vurim A, Mukhamedova N, Baklanova Y, et al. (2022) Information and analytical system for processing of research results to justify the safety of atomic energy. *Appl Sci* 12: 9705. https://doi.org/10.3390/app12199705
24. Skakov M, Toleubekov K, Baklanov V, et al. (2022) The method of corium cooling in a core catcher of a light-water nuclear reactor. *Eurasian Phys Tech J* 19: 69–77. https://doi.org/10.31489/2022No3/69-77
25. Skakov M, Baklanov V, Akaev A, et al. (2023) On the possibility of forming a corium pool by induction heating in a core catcher of the Lava-B facility. *Appl Sci* 13: 2480. https://doi.org/10.3390/app13042480
26. Kato M, Nagasaka H, Vasilyev Y, et al. (2000) COTELS fuel coolant interaction tests under ex-vessel conditions. Proceedings of the JAERI-Conference, 36–42.
27. Bekmuldin M, Skakov M, Baklanov V, et al. (2023) Experimental simulation of decay heat of corium at the Lava-B test-bench. *Nucl Technol* 210: 46–54 https://doi.org/10.1080/00295450.2023.2226539

AIMS Press

© 2024 the Author(s), licensee AIMS Press. This is an open access article distributed under the terms of the Creative Commons Attribution License (http://creativecommons.org/licenses/by/4.0)